HHS Public Access

Author manuscript

Transplantation. Author manuscript; available in PMC 2016 September 01.

Published in final edited form as:

Transplantation. 2015 September ; 99(9): e132–e139. doi:10.1097/TP.0000000000000618.

Use of [^{18}F]FDG PET to Monitor The Development of Cardiac Allograft Rejection

Kevin P. Daly, MD[1,2,3], **Jason L. J. Dearling, PhD**[4,5], **Tatsuichiro Seto, MD**[1,3,6], **Patricia Dunning**[4], **Frederic Fahey, ScD**[4,5], **Alan B. Packard, PhD**[4,5], and **David M. Briscoe, MD**[1,3,6]

[1]Transplant Research Program, Boston Children's Hospital, Boston, MA

[2]Department of Cardiology, Boston Children's Hospital, Boston, MA

[3]Department of Pediatrics, Harvard Medical School, Boston, MA

[4]Division of Nuclear Medicine and Molecular Imaging, Department of Radiology, Boston Children's Hospital, Boston, MA

[5]Department of Radiology, Harvard Medical School, Boston, MA

[6]Division of Nephrology, Department of Medicine, Boston Children's Hospital, Boston, MA

Abstract

Background—Positron Emission Tomography (PET) has the potential to be a specific, sensitive and quantitative diagnostic test for transplant rejection. To test this hypothesis, we evaluated ^{18}F-labeled fluorodeoxyglucose ([^{18}F]FDG) and ^{13}N-labeled ammonia ([^{13}N]NH_3) small animal PET imaging in a well-established murine cardiac rejection model.

Methods—Heterotopic transplants were performed using minor MHC mismatched B6.C-H2^{bm12} donor hearts in C57BL/6(H-2^{b}) recipients. C57BL/6 donor hearts into C57BL/6 recipients served as isograft controls. [^{18}F]FDG PET imaging was performed weekly between post-transplant days 7 and 42 and the percent injected dose was computed for each graft. [^{13}N]NH_3 imaging was performed to evaluate myocardial perfusion.

Results—There was a significant increase in [^{18}F]FDG uptake in allografts from day 14 to day 21 (1.6% to 5.2%; P<0.001) and uptake in allografts was significantly increased on post-transplant days 21 (5.2% vs. 0.9%; P=0.005) and 28 (4.8% vs. 0.9%; P=0.006) compared to isograft controls.

Address for Correspondence: Kevin P. Daly, MD, Transplant Research Program, And the Department of Cardiology, Boston Children's Hospital, 300 Longwood Avenue, Boston, MA 02115, Telephone: 617-355-6329, Fax: 617-734-9930, kevin.daly@childrens.harvard.edu.

Kevin P. Daly, MD, Transplant Research Program, And the Department of Cardiology, Boston Children's Hospital, 300 Longwood Avenue, Boston, MA 02115

David M. Briscoe, MD, Tatsuichiro Seto, MD, Transplant Research Program, And the Division of Nephrology, Boston Children's Hospital, 300 Longwood Ave, Boston, MA 02115

Alan B. Packard, PhD, Jason L. J. Dearling, PhD, Frederic Fahey, ScD, Patricia Dunning, Department of Radiology, Boston Children's Hospital, 300 Longwood Ave, Boston, MA 02115

Authorship

K.P.D., J.L.J.D., F.F., A.B.P. and D.M.B contributed to the research design. K.P.D., J.L.J.D., T.S., P.D., and A.B.P. participated in performance of the research. K.P.D. wrote the manuscript. K.P.D., J.L.C.D, F.F., A.B.P, and D.M.B participated in data analysis and editing of the paper. A.B.P. and D.M.B. served as co-senior authors for this work.

Conflicts of Interest

The authors declare no conflicts of interest.

Furthermore, [^{18}F]FDG uptake correlated with an increase in rejection within allografts between days 14 and 28 post-transplant. Finally, the uptake of [^{13}N]NH_3 was significantly lower relative to the native heart in allografts with chronic vasculopathy compared to isograft controls on day 28 (P=0.01).

Conclusions—PET imaging with [^{18}F]FDG can be used following transplantation to monitor the evolution of rejection. In addition, decreased uptake of [^{13}N]NH_3 in rejecting allografts may be reflective of decreased myocardial blood flow. These data suggest that combined [^{18}F]FDG and [^{13}N]NH_3 PET imaging could be used as a non-invasive, quantitative technique for serial monitoring of allograft rejection and has potential application in human transplant recipients.

Keywords

Heart transplantation; PET Imaging; Rejection; Mice; Heterotopic Transplantation; Translational Research

INTRODUCTION

Acute cardiac allograft rejection involves a marked inflammatory reaction characterized by the recruitment of leukocytes and intense cellular and humoral immune responses to the graft. In contrast, chronic rejection is an insidious process involving delayed type hypersensitivity mechanisms, and it is characterized by mononuclear cell infiltration, cardiac allograft vasculopathy (CAV), and progressive fibrosis (1). Surveillance of recipients for evidence of allograft rejection and CAV through non-invasive imaging has emerged as a key area for improvement in post-transplant care. Early detection of allograft damage is of paramount importance to clinicians as rejection and CAV are associated with graft loss and mortality (2–4).

While endomyocardial biopsy remains the gold standard for identification of rejection, it provides only ordinal data on the degree of rejection, is invasive, is prone to sampling error, and has limited interobserver reproducibility (5, 6). The glucose analogue 2-[^{18}F]fluoro-2-deoxy-D-glucose ([^{18}F]FDG) can be used to quantify glucose uptake and glycolytic activity in native and transplanted hearts (7–9). Fluorine-18-FDG also provides a measure of local inflammatory activity through uptake by immune cells (10). In cardiac transplants undergoing rejection, increased uptake of [^{18}F]FDG could provide a non-invasive, quantitative measure of increasing numbers of inflammatory infiltrates and thus support the diagnosis of evolving rejection in clinical care, clinical trials, and research applications.

Microvascular injury is a characteristic component of cellular and humoral rejection and leads to changes in local blood flow patterns resulting in local tissue hypoxia (11, 12). Microvascular disease is an important component of the pathophysiology of CAV and is related to patient outcome (13). Both micro and macrovascular changes in blood flow in the heart can be quantified using a myocardial perfusion tracer, such as [^{13}N]NH_3; Uptake and retention by the myocardium is reflective of metabolic trapping and flow-dependent back diffusion, respectively (14).

In this study, we used a well-characterized minor-MHC mismatched heterotopic cardiac transplant model to evaluate whether [^{18}F]FDG PET could be used to monitor the evolution of inflammatory infiltrates and [^{13}N]NH_3 could be used as a monitor of microvascular loss (15).

RESULTS

Trends in [^{18}F]FDG Uptake in Fully MHC Matched Isografts Over Time

[^{18}F]FDG uptake in transplanted isografts (C57BL/6(H-2^b) donors → C57BL/6(H-2^b) recipients) on day 7 was not different from uptake in the native mouse heart and represented 4.1% of the injected dose. The percent injected dose in isografts decreased to 1.6% at day 14 before reaching a minimum value of less than 1% on days 21–42 (Figure 1 & 2). Compared to uptake in the animal's native heart, isografts showed significantly less [^{18}F]FDG uptake throughout the study (P=0.03). H&E staining of histologic specimens from isografts did not show any lymphocytic infiltrates or evidence of rejection on days 7, 14, 28, and 42 and were assigned ISHLT Cellular Rejection Grade 0R (Figure 3A).

Rejecting Allografts Have Increased [^{18}F]FDG Uptake at 21 and 28 Days Post-Transplant Compared to Non-rejecting Isograft Controls

[^{18}F]FDG uptake in transplanted allografts (B6.C-H2^{bm12} donors → C57BL/6(H-2^b) recipients) increased from day 7 through 42 (P< 0.001). When compared to isograft controls at similar time points, the percent injected dose of [^{18}F]FDG in the allografts was significantly higher (P<0.001) (Figure 2). Bonferroni-corrected pairwise comparisons revealed significant differences in percent injected dose of [^{18}F]FDG between allografts and isograft controls on day 21 (5.2% vs. 0.9%; P=0.005) and day 28 (4.8% vs. 0.9%; P=0.006) (Figure 2). Within allografts, the percent injected dose decreased from 3.6% on day 7 to 1.7% on day 14 before increasing to 5.2% on day 21 and 4.8% on day 28 (Figure 2), a time when rejection increased within allografts from an ISHLT Grade 1R on day 7 to Grade 2R on day 14 and grade 3R on day ≥ 28 (Figure 3). The percent injected dose decreased to 1.7% and 2.7% on days 35 and 42 respectively. Bonferroni-corrected individual pairwise comparisons were significant between days 14 and 21 (+3.6%; P=0.002), days 14 and 28 (+3.1%; P=0.02) and days 21 and 35 (−3.5%; P=0.04). H&E staining and immunohistochemical staining for CD45 confirmed significant inflammatory infiltrates by day 28 consistent with the possibility that the increase in [^{18}F]FDG PET uptake within the transplanted allografts is reflective of increasing degrees of rejection (Figure 3).

Treatment of animals with anti-CD40L or rapamycin leads to reduced [^{18}F]FDG uptake

Allograft recipients were treated with the co-stimulatory antagonist anti-CD40L (MR1, 200 mcg daily on days 0, 2, and 4), which decreases effector responses and results in prolonged allograft survival. As expected (16), we found that anti-CD40L antibody treatment led to near complete inhibition of rejection, as assessed by histology on day 28 post-transplantation (Figure 4). Uptake of [^{18}F]FDG was significantly lower in anti-CD40L treated allograft recipients compared to untreated allograft recipients across all time points (P=0.006; Figure 5). Bonferroni- corrected individual pairwise comparisons were significantly lower at day 21 (0.8% vs. 5.2%; P=0.003) and day 28 (0.7% vs. 4.8%; P=0.001).

We also evaluated [^{18}F]FDG uptake in recipients treated with low dose rapamycin (0.3 mg/kg/day IP given 3 times a week). Again, we observed lower uptake of [^{18}F]FDG in the animals treated with rapamycin; however, the decrease in [^{18}F]FDG uptake did not reach statistical significance (Figure 5; day 7: 1.5% rapamycin vs. 3.6% untreated; day 14: 1.3% vs. 1.6%; day 21: 2.8% vs. 5.2%). Consistent with this result, histology from day 28 showed incomplete inhibition of the rejection response (Figure 4).

Relative Uptake of [^{13}N]NH_3 is Decreased in Rejecting Allografts with CAV

[^{13}N]NH_3 PET imaging was performed in allograft and isograft recipients on post-transplant day 28 to measure differences in myocardial blood flow. Elastin stains from allografts harvested on day 28 demonstrated a significantly higher CAV burden (average percent vessel occlusion 56% in allografts vs. 4% in isografts; $P<0.01$). Also, the number of vessels present within allografts (6.9 vessels/section) was less than that observed in isografts (11.7 vessels/section; $P<0.01$). The ratio of [^{13}N]NH_3 uptake in the transplanted heart to that in the animal's native heart was significantly lower in untreated allograft recipients compared to isograft recipients suggesting that [^{13}N]NH_3 PET can identify a relative decrease in myocardial blood flow in rejecting allografts (-1.56 ± 0.17 vs. -0.24 ± 0.32; $P=0.01$).

Effect of Diet on [^{18}F]FDG Uptake in Native Hearts

Twenty animals were placed on a custom-made low-carbohydrate diet 5 days prior to undergoing a [^{18}F]FDG PET scan in an attempt to shift myocardial energy metabolism away from glucose. Uptake of [^{18}F]FDG by the animal's native heart was not different between animals maintained on a low carbohydrate diet compared to animals maintained on a normal carbohydrate rich diet (Low carbohydrate (N=20): 2.7% ± 0.9 vs. Standard diet (N=35): 2.7% ± 1.3; $P=0.97$).

DISCUSSION

In this study, we demonstrate that non-invasive PET imaging can be used to detect rejection in a minor MHC mismatched model of cardiac allograft rejection. Using [^{18}F]FDG as a tracer, we demonstrate increased [^{18}F]FDG uptake in rejecting allografts compared to non-rejecting isograft controls. The [^{18}F]FDG signal peaks in allografts in association with increased leukocytic infiltration at 3–4 weeks post-transplantation in this well established pre-clinical model. We also find that [^{18}F]FDG uptake is reduced to levels seen in non-rejecting controls in allograft recipients treated with anti-CD40L. Finally, our data show that [^{13}N]NH_3 PET imaging can identify lower relative myocardial blood flow in chronically rejecting allografts compared to non-rejecting controls. Collectively, these findings indicate that both [^{18}F]FDG and [^{13}N]NH_3 PET imaging have potential application as a non-invasive, quantitative technique for the evaluation of allograft rejection. While this technology has potential for the serial monitoring of inflammatory infiltrates and rejection in animal models, we suggest that it is possible to translate this technology to human transplant recipients in the future.

PET imaging allows for serial, specific, non-invasive, and quantitative imaging of physiologic and pathophysiologic processes by incorporating a positron emitting nuclide

within a physiologically relevant molecule. [^{18}F]FDG is a widely used tracer that is taken up by all cells metabolizing glucose including leukocytes, myocardial cells, and neuronal cells. Prior work has shown that [^{18}F]FDG uptake is high in the transplanted myocardium in a heterotopic rat model of acute cardiac allograft rejection (17). However, in that study [^{18}F]FDG uptake was measured after the animals were sacrificed and was not evaluated serially or in real time within each transplanted animal. In our study, we show that serial [^{18}F]FDG-PET imaging can be performed in the same recipient mouse to monitor the evolution of the rejection process. Furthermore, we show that [^{18}F]FDG uptake correlates with histologically proven rejection. In this murine model the sensitivity of [^{18}F]FDG PET for detection of Grade 1R and 2R rejection is limited. We have, however, demonstrated that PET imaging can be used to monitor the evolution of rejection and we hope that this will stimulate the testing of novel radiopharmaceuticals for this indication.

Our rationale for using [^{18}F]FDG PET to monitor rejection is that activated leukocytes present in the rejecting heart should take up [^{18}F]FDG leading to an increased signal, similar to what has been shown in rejection of skin grafts (18). An alternative hypothesis is that rejection shifts myocardial metabolism towards glucose in general, or increases uptake of [^{18}F]FDG relative to glucose, resulting in increased myocardial signal (8). It is possible that left ventricular dysfunction, which is expected to occur in the context of rejection, could increase [^{18}F]FDG uptake. We believe this to be unlikely since studies have shown that dilated cardiomyopathy patients with ventricular dysfunction can have decreased [^{18}F]FDG uptake (19), counter to what we find in rejecting allografts. Regardless of whether [^{18}F]FDG is taken up by leukocytes or whether rejection alters myocardial uptake of [^{18}F]FDG, the findings demonstrate that [^{18}F]FDG PET has the potential not only to identify rejection, but also to monitor its evolution.

It is interesting to note that both isografts and allografts demonstrate increased [^{18}F]FDG uptake in the heterotopic transplanted heart 7 days post-transplant. This increased uptake is abolished by immunosuppression with anti-CD40L and attenuated by rapamycin. The cause of this phenomenon is not entirely clear, but it is most likely related to differing degrees of ischemia-reperfusion injury. Several studies have shown that adaptive and innate immune responses are important for the development of ischemia reperfusion injury and that targeting the immune response inhibits leukocyte infiltration and organ injury (20, 21). It is likely that [^{18}F]FDG PET can identify immune responses that coincide with ischemia-reperfusion injury, a phenomenon which is reduced in animals treated with anti-CD40L or rapamycin. Alternatively, the increased myocardial uptake of [^{18}F]FDG at day 7 may be due to the transition in myocardial energy expenditure from a working heart to a non-working heart. Myocardial energy expenditure is proportional to the sum of the area within the pressure-volume loop and the potential energy stored in the muscle and is therefore dependent upon contractility, ventricular volume and arterial pressure (22). In the heterotopic heart transplant model used in this study, the transplanted heart performs no significant left ventricular pressure-volume work and only minimal myocardial metabolic activity is required in order to generate potential energy. Zehr *et al.* have previously shown that a non-working canine heterotopic heart transplant model has low baseline myocardial oxygen consumption and energy metabolism using PET imaging (23). For these reasons, the

low [^{18}F]FDG uptake in the non-rejecting controls is expected. Hoff *et al.* increased basal myocardial work in a rat heterotopic heart transplant model by creating aortic regurgitation and forcing the left ventricle to perform pressure-volume work (24). In that study, increased [^{18}F]FDG uptake was present in rejecting hearts compared to non-rejecting controls despite the increase in basal [^{18}F]FDG uptake.

When considering translation of these findings to human heart transplant recipients, it is important to understand how differences in basal myocardial uptake of [^{18}F]FDG in a working human heart may affect the ability to detect rejection. Basal myocardial [^{18}F]FDG uptake has been shown to be higher in human transplant recipients than in non-transplanted control patients (7). In addition, there is significant baseline variation in myocardial uptake of [^{18}F]FDG between non-transplanted adults, even when controlling for blood glucose levels, age, and duration of fasting (9, 25). Such variability would make attribution of changes in [^{18}F]FDG uptake to rejection more difficult. In an attempt to minimize basal uptake of [^{18}F]FDG in the myocardium, we fed mice a low carbohydrate diet (5% of calories from carbohydrates) with the goal of shifting myocardial metabolism to exclusive use of free fatty acids. This was based on data from several human studies showing the ability to minimize the background myocardial uptake of [^{18}F]FDG with a low carbohydrate diet combined with fasting (26, 27). Despite the use of a low carbohydrate diet, we did not see any difference in myocardial uptake of [^{18}F]FDG in native murine hearts when compared to mice on a standard carbohydrate diet (60% of calories). Data from other studies have shown that fasting mice for 12 hours prior to scanning decreases myocardial uptake of [^{18}F]FDG (28).

[^{18}F]PET imaging may serve to decrease, but not eliminate, the need for protocol biopsies. Similar to the use of other biomarkers, it is likely that a negative PET scan could allow for a decreased biopsy frequency, whereas a positive PET would trigger a biopsy. For instance, the AlloMap (CareDx, Brisbane, CA) can be used to reduce the frequency of biopsy without altering clinical outcomes (29). In addition, sampling error can be an issue with endomyocardial biopsy and pathological interpretation of biopsies is subject to bias and significant intra-observer variability (30, 31). We believe that [^{18}F]PET is less subject to sampling bias and provides a quantitative means to assess rejection throughout the entire graft.

Microvascular injury and capillary loss is a well-characterized aspect of the pathophysiology of acute and chronic rejection, which led to the hypothesis that a quantitative myocardial blood flow tracer could monitor the degree of microvascular injury. Our pilot data suggest that [^{13}N]NH_3 can identify decreases in myocardial blood flow seen in association with histologically demonstrated CAV. However, [^{13}N]NH_3 requires an onsite cyclotron for production due to its extremely short half-life (10 minutes) leading to increased cost per dose. Nevertheless, we suggest that myocardial flow quantification, perhaps with a different tracer, will increase sensitivity and specificity for the non-invasive imaging of rejection.

We have demonstrated that rejection can be detected in a heterotopic mouse model of chronic allograft rejection using [^{18}F]FDG PET. PET imaging has significant potential to serve as a useful research tool for the monitoring and quantification of allograft rejection in

animal models and in therapeutic trials. Translation of this technology to the clinical setting remains appealing, but baseline variability in myocardial [^{18}F]FDG uptake may ultimately limit the sensitivity of this test for identification of allograft rejection. Development of a radiotracer that is specific to the immune response and/or to the myocardial injury that occurs during the rejection process would be ideal. Nevertheless, this study opens up the area of PET imaging as a non-invasive means to detect, quantify, and follow allograft rejection.

MATERIALS & METHODS

Mouse Heterotopic Transplantation Model

B6.C-H2^{bm12} and C57BL/6(H-2^{b}) mice aged 6–8 weeks were purchased from The Jackson Laboratory (Bar Harbor, ME). Hearts from B6.C-H2^{bm12} mice were transplanted into the abdomen of C57BL/6(H-2^{b}) mice to create a model of minor-MHC mismatched allograft transplants as previously described. (15, 32) Hearts from C57BL/6(H-2^{b}) mice transplanted into C57BL/6(H-2^{b}) mice served as isograft transplant controls. Mice were anesthetized using ketamine (80–100 mg/kg IP) and xylazine (5–10 mg/kg IP) for the procedure. Graft function was assessed by palpation. None of the grafts ceased to function during the study.

Treatment of Allograft Rejection

Unless specified, no treatment was given to the recipient mice to prevent allograft rejection. In order to determine if rejection was the cause of changes in [^{18}F]FDG uptake in the transplanted hearts, five C57BL/6(H-2^{b}) mice who received B6.C-H2^{bm12} allografts were treated with anti-CD40L antibody (200 μg IP injection on post-transplant days 0, 2, and 4). Animals underwent [^{18}F]FDG PET imaging on post-transplant days 7, 14, 21, and 28 and were sacrificed on day 28 for histology after they were confirmed to have graft function by palpation. In addition, three C57BL/6(H-2^{b}) mice who received B6.C-H2^{bm12} allografts were treated with rapamycin (0.3 mg/kg/day given 3 times a week; a gift of Wyeth Pharmaceuticals Company, Philadelphia, PA) and [^{18}F]FDG PET imaging was performed on post-transplant days 7, 14, and 21. Animals were sacrificed on day 28 for histology.

[^{18}F]FDG Positron Emission Tomography

[^{18}F]FDG PET imaging was performed weekly between post-transplant days 7 and 42 with a minimum of 3 animals of each transplant type imaged at every time point. Animals were injected with 100 μL of [^{18}F]FDG (5.6–7.4 MBq, 150–200 μCi) intravenously via the tail vein. After tracer administration, the animals were placed back in their cage for 30 minutes to allow for radiotracer uptake by cells. The animals were then anesthetized with isoflurane and PET data were collected for 15 (^{13}N) or 30 (^{18}F) minutes using a Siemens Focus 120 microPET scanner (Siemens Medical Solutions USA, Inc.). Following reconstruction (OSEM2D after Fourier rebinning), images were analyzed using AMIDE (33). Ellipsoid volumes of interest (VOI) were placed around the native heart and the transplanted hearts as shown in Figure 1. Ventricular blood pools were not excluded from the VOI but care was taken to exclude the bladder. The total amount of radioactivity in each VOI was computed. For [^{18}F]FDG imaging, the percent injected dose was computed by normalizing the decay-corrected injected activity. Imaging with [^{13}N]NH_3 was performed in a similar manner. Due

to the short half-life of ^{13}N (10 minutes compared to 110 minutes for ^{18}F), the same injected dose was not consistently obtained. As a result, a ratio of total radioactivity in the transplanted heart to the native heart was calculated and reported as a relative measure of myocardial perfusion.

Low-Carbohydrate Mouse Diet

Mice received standard feed (Prolab Isopro RMH 3000; LabDiet, St. Louis, MO) which provides 60% of calories from carbohydrates, 14% from fat, and 26% from protein sources. After significant [^{18}F]FDG uptake was noted in the native heart, mice were trialed on a low-carbohydrate diet (Dyets, Bethlehem, PA) to determine if dietary changes could induce a ketogenic state and decrease active glucose transport into the myocardial cells. The diet provided a standard caloric density with only 5% of calories from carbohydrate sources, 60% from fat and 35% from protein. Animals were placed on the special feed 5 days prior to [^{18}F]FDG injection and returned to a standard diet following each scan.

Histologic Examination

Cardiac grafts were harvested at weekly time points (day 7, 14, 21, 28, 35, 42) after transplantation. Hearts were divided into three pieces. One piece was fixed in 10% buffered formalin for 24–48 hours, embedded in paraffin, cut, and stained with hematoxylin and eosin (H&E) for evaluation of rejection according to the 2005 ISHLT rejection grading scale (5) or elastin for evaluation of CAV as previously described (34). A second piece was frozen in optimal cutting temperature (OCT) compound on dry ice and stored at −80°C for later immunohistochemical staining. Four micron sections were incubated with rat anti-mouse CD45 (1:100 dilution, BD Pharmingen, San Diego, CA), and subsequently with a 1:40 dilution of donkey anti-rat peroxidase-conjugated secondary antibody (Jackson Immunoresearch, West Grove, PA); staining was detected by incubation with 3-amino 9-ethylcarbazole (AEC). Sections were then counter stained with hematoxylin and mounted for histological analysis.

Statistics

Two-way ANOVA was used to compare percent injected dose of [^{18}F]FDG in the region of interest between groups and across time points. Standard two-group Student T-tests were used to generate P-values for individual comparisons. An ANOVA P-value of less than 0.05 was considered significant. Reported P-values have been multiplied by the total number of comparisons in order to incorporate the Bonferroni correction and maintain the family wise threshold for alpha error at 0.05. The Wilcoxon rank-sum test was used for two-group comparison of variables with a skewed distribution. Ratios were log transformed and compared using the Student T-test. Time points for the various investigations were normalized to seven-day intervals post-transplant plus or minus two days. STATA 10.0 (College Station, TX) software was used for all statistical comparisons.

Statement of Regulatory Compliance

All animals used in this study were treated in a humane manner according to a research protocol approved by the Boston Children's Hospital Institutional Animal Care and Use Committee (09-04-1336R).

Acknowledgments

Research Support

This work was funded in part by NIH grants UL1 RR 025758 (Harvard Catalyst to K.P.D., D.M.B. and A.B.P.), and 3R01AI046756-10S1 (to D.M.B.) and the Children's Hospital Radiology Foundation (to A.B.P. and J.L.J.D.). In addition, K.P.D. was supported by NIH grants T32 HL07572, K12HD052896-06, and the Boston Children's Hospital Cardiac Transplant and Education Fund.

Abbreviations

[^{18}F]FDG	^{18}F-labeled fluorodeoxyglucose
[^{13}N]NH_3	^{13}N-labeled ammonia
AEC	3-amino 9-ethylcarbazole
CAV	cardiac allograft vasculopathy
IP	intraperitoneal
OCT	optimal cutting temperature
PET	positron emission tomography
VOI	volume of interest

References

1. Libby P, Pober JS. Chronic rejection. Immunity. 2001; 14(4):387. [PubMed: 11336684]
2. Webber SA, Naftel DC, Parker J, et al. Late rejection episodes more than 1 year after pediatric heart transplantation: risk factors and outcomes. J Heart Lung Transplant. 2003; 22(8):869. [PubMed: 12909466]
3. Phelps CM, Tissot C, Buckvold S, et al. Outcome of acute graft rejection associated with hemodynamic compromise in pediatric heart transplant recipients. Pediatr Cardiol. 2011; 32(1):1. [PubMed: 20963408]
4. Yamani MH, Haji SA, Starling RC, et al. Myocardial ischemic-fibrotic injury after human heart transplantation is associated with increased progression of vasculopathy, decreased cellular rejection and poor long-term outcome. J Am Coll Cardiol. 2002; 39(6):970. [PubMed: 11897438]
5. Stewart S, Winters GL, Fishbein MC, et al. Revision of the 1990 working formulation for the standardization of nomenclature in the diagnosis of heart rejection. J Heart Lung Transplant. 2005; 24(11):1710. [PubMed: 16297770]
6. Angelini A, Andersen CB, Bartoloni G, et al. A web-based pilot study of inter-pathologist reproducibility using the ISHLT 2004 working formulation for biopsy diagnosis of cardiac allograft rejection: the European experience. J Heart Lung Transplant. 2011; 30(11):1214. [PubMed: 21816625]
7. Rechavia E, de Silva R, Kushwaha SS, et al. Enhanced myocardial 18F-2-fluoro-2-deoxyglucose uptake after orthotopic heart transplantation assessed by positron emission tomography. J Am Coll Cardiol. 1997; 30(2):533. [PubMed: 9247529]
8. Taegtmeyer H, Doenst T. F-18 FDG uptake in transplanted heart. J Am Coll Cardiol. 1998; 31(6): 1441. [PubMed: 9581748]

9. de Groot M, Meeuwis AP, Kok PJ, Corstens FH, Oyen WJ. Influence of blood glucose level, age and fasting period on non-pathological FDG uptake in heart and gut. Eur J Nucl Med Mol Imaging. 2005; 32(1):98. [PubMed: 15605289]
10. Kubota R, Yamada S, Kubota K, Ishiwata K, Tamahashi N, Ido T. Intratumoral distribution of fluorine-18-fluorodeoxyglucose in vivo: high accumulation in macrophages and granulation tissues studied by microautoradiography. J Nucl Med. 1992; 33(11):1972. [PubMed: 1432158]
11. Bruneau S, Woda CB, Daly KP, et al. Key Features of the Intragraft Microenvironment that Determine Long-Term Survival Following Transplantation. Front Immunol. 2012; 3(54):54. [PubMed: 22566935]
12. Steegh FM, Gelens MA, Nieman FH, et al. Early loss of peritubular capillaries after kidney transplantation. J Am Soc Nephrol. 2011; 22(6):1024. [PubMed: 21566051]
13. Hiemann NE, Wellnhofer E, Knosalla C, et al. Prognostic impact of microvasculopathy on survival after heart transplantation: evidence from 9713 endomyocardial biopsies. Circulation. 2007; 116(11):1274. [PubMed: 17709643]
14. Schelbert HR, Phelps ME, Huang SC, et al. N-13 ammonia as an indicator of myocardial blood flow. Circulation. 1981; 63(6):1259. [PubMed: 7226473]
15. Nagano H, Mitchell RN, Taylor MK, Hasegawa S, Tilney NL, Libby P. Interferon-gamma deficiency prevents coronary arteriosclerosis but not myocardial rejection in transplanted mouse hearts. J Clin Invest. 1997; 100(3):550. [PubMed: 9239401]
16. Larsen CP, Alexander DZ, Hollenbaugh D, et al. CD40-gp39 interactions play a critical role during allograft rejection. Suppression of allograft rejection by blockade of the CD40-gp39 pathway. Transplantation. 1996; 61(1):4. [PubMed: 8560571]
17. Hoff SJ, Stewart JR, Frist WH, et al. Noninvasive detection of heart transplant rejection with positron emission scintigraphy. Ann Thorac Surg. 1992; 53(4):572. [PubMed: 1554263]
18. Heelan BT, Osman S, Blyth A, Schnorr L, Jones T, George AJ. Use of 2-[18F]fluoro-2-deoxyglucose as a potential agent in the prediction of graft rejection by positron emission tomography. Transplantation. 1998; 66(8):1101. [PubMed: 9808498]
19. Yamaguchi H, Hasegawa S, Yoshioka J, et al. Characteristics of myocardial 18F-fluorodeoxyglucose positron emission computed tomography in dilated cardiomyopathy and ischemic cardiomyopathy. Ann Nucl Med. 2000; 14(1):33. [PubMed: 10770578]
20. Huang Y, Rabb H, Womer KL. Ischemia-reperfusion and immediate T cell responses. Cell Immunol. 2007; 248(1):4. [PubMed: 17942086]
21. Takada M, Chandraker A, Nadeau KC, Sayegh MH, Tilney NL. The role of the B7 costimulatory pathway in experimental cold ischemia/reperfusion injury. J Clin Invest. 1997; 100(5):1199. [PubMed: 9276737]
22. Suga H. Global cardiac function: mechano-energetico-informatics. J Biomech. 2003; 36(5):713. [PubMed: 12695001]
23. Zehr KJ, Wong CY, Chin B, et al. Comparison of myocardial oxygen consumption using 11C acetate positron emission tomography scanning in a working and non-working heart transplant model. Eur J Cardiothorac Surg. 2001; 19(1):74. [PubMed: 11163564]
24. Hoff SJ, Stewart JR, Frist WH, et al. Noninvasive detection of acute rejection in a new experimental model of heart transplantation. Ann Thorac Surg. 1993; 56(5):1074. [PubMed: 8239802]
25. Kaneta T, Hakamatsuka T, Takanami K, et al. Evaluation of the relationship between physiological FDG uptake in the heart and age, blood glucose level, fasting period, and hospitalization. Ann Nucl Med. 2006; 20(3):203. [PubMed: 16715951]
26. Cheng VY, Slomka PJ, Ahlen M, Thomson LE, Waxman AD, Berman DS. Impact of carbohydrate restriction with and without fatty acid loading on myocardial 18F-FDG uptake during PET: A randomized controlled trial. J Nucl Cardiol. 17(2):286. [PubMed: 20013165]
27. Williams G, Kolodny GM. Suppression of myocardial 18F-FDG uptake by preparing patients with a high-fat, low-carbohydrate diet. AJR Am J Roentgenol. 2008; 190(2):W151. [PubMed: 18212199]

28. Verberne HJ, Sloof GW, Beets AL, Murphy AM, van Eck-Smit BL, Knapp FF. 125I-BMIPP and 18F-FDG uptake in a transgenic mouse model of stunned myocardium. Eur J Nucl Med Mol Imaging. 2003; 30(3):431. [PubMed: 12722739]

29. Pham MX, Teuteberg JJ, Kfoury AG, et al. Gene-expression profiling for rejection surveillance after cardiac transplantation. N Engl J Med. 2010; 362(20):1890. [PubMed: 20413602]

30. Yang HM, Lai CK, Gjertson DW, et al. Has the 2004 revision of the International Society of Heart and Lung Transplantation grading system improved the reproducibility of the diagnosis and grading of cardiac transplant rejection? Cardiovasc Pathol. 2009; 18(4):198. [PubMed: 18619859]

31. Crespo-Leiro MG, Zuckermann A, Bara C, et al. Concordance among pathologists in the second Cardiac Allograft Rejection Gene Expression Observational Study (CARGO II). Transplantation. 2012; 94(11):1172. [PubMed: 23222738]

32. Corry RJ, Winn HJ, Russell PS. Heart transplantation in congenic strains of mice. Transplant Proc. 1973; 5(1):733. [PubMed: 4572133]

33. Loening AM, Gambhir SS. AMIDE: a free software tool for multimodality medical image analysis. Mol Imaging. 2003; 2(3):131. [PubMed: 14649056]

34. Womer KL, Stone JR, Murphy B, Chandraker A, Sayegh MH. Indirect allorecognition of donor class I and II major histocompatibility complex peptides promotes the development of transplant vasculopathy. J Am Soc Nephrol. 2001; 12(11):2500. [PubMed: 11675428]

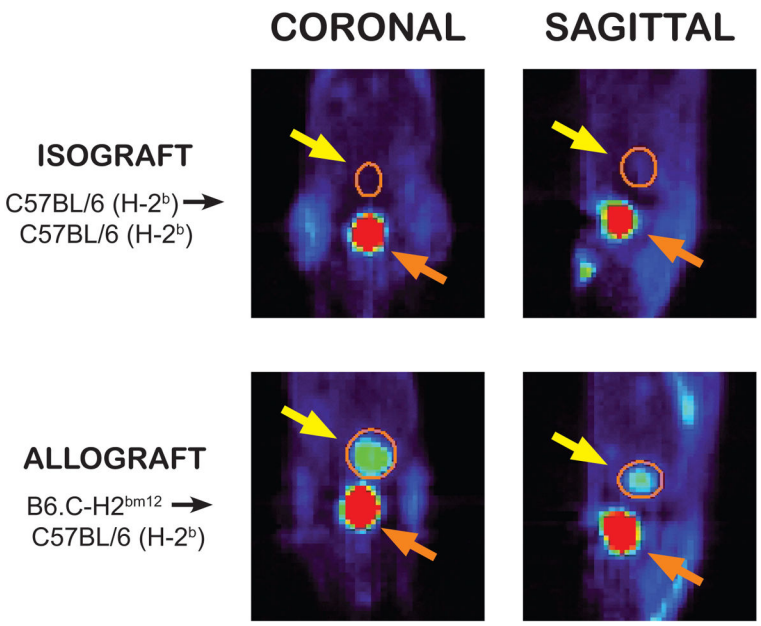

Figure 1.

A representative [^{18}F]FDG positron emission tomography scan of a mouse recipient of a heterotopic heart transplant on post-transplant day 28 is displayed in the coronal and sagittal planes. The heterotopic heart transplant is circled in orange and highlighted with the yellow arrow. The non-rejecting fully MHC matched isograft heart shows minimal [^{18}F]FDG uptake compared to the rejecting minor-MHC mismatched allograft heart. The bladder (orange arrow) is visualized inferior to the transplanted heart with significant [^{18}F]FDG activity in both animals, reflective of [^{18}F]FDG excretion in the urine.

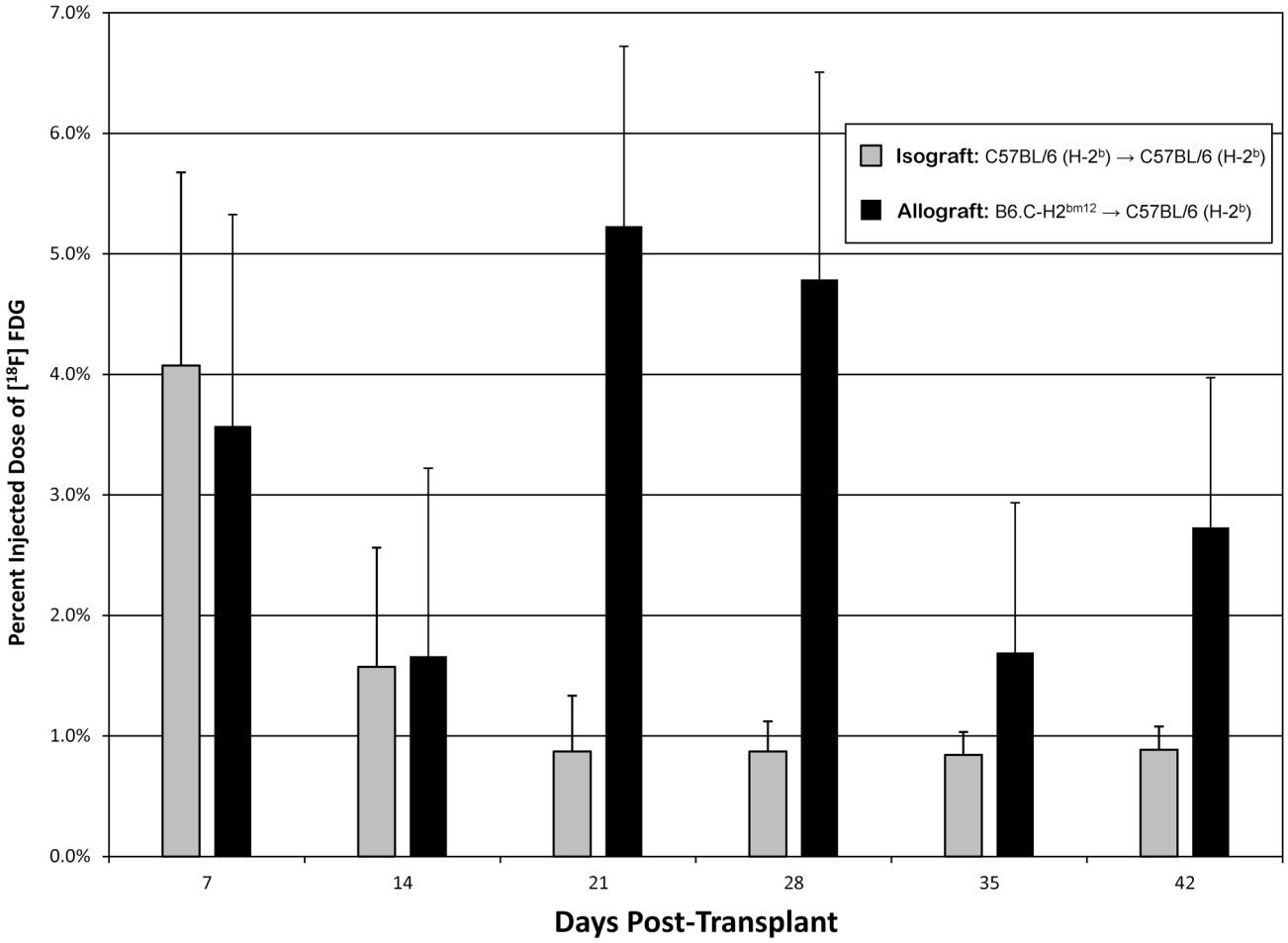

Figure 2.

The percent injected dose of [^{18}F]FDG within the transplanted heart in fully MHC matched isograft and minor-MHC mismatched allograft is displayed. Error bars represent the standard deviation of measurements within each group. After correcting for multiple comparisons, significant differences were observed between percent injected dose of [^{18}F]FDG between allografts and isografts at post-transplant day 21 (P=0.005) and 28 (P=0.006).

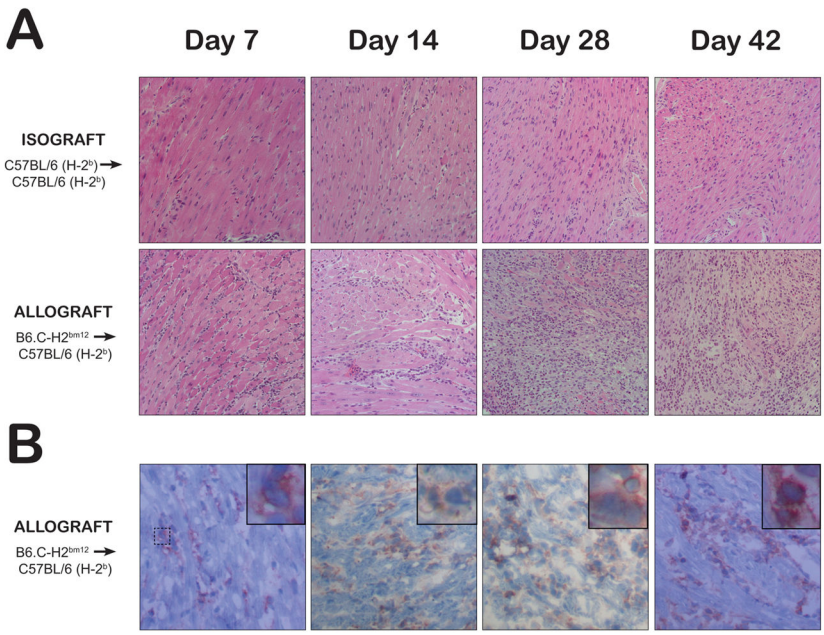

Figure 3.

Representative histology of transplanted hearts from untreated isograft and allograft recipients at day 7, 14, 28, and 42 post-transplant is displayed. **(A)** The upper and middle rows show representative H&E stained hearts. **(B)** The lower row displays representative immunohistochemical staining of CD45-positive infiltrates confirming that the interstitial cells are lymphocytes. There is minimal lymphocytic infiltration in isograft hearts (ISHLT Grade 0R) while allografts show interstitial lymphocytes on days 7 (Grade 1R) and 14 (Grade 2R) with diffuse sheets of activated lymphocytes with associated cardiomyocyte damage seen on days 28 and 42 (Grade 3R).

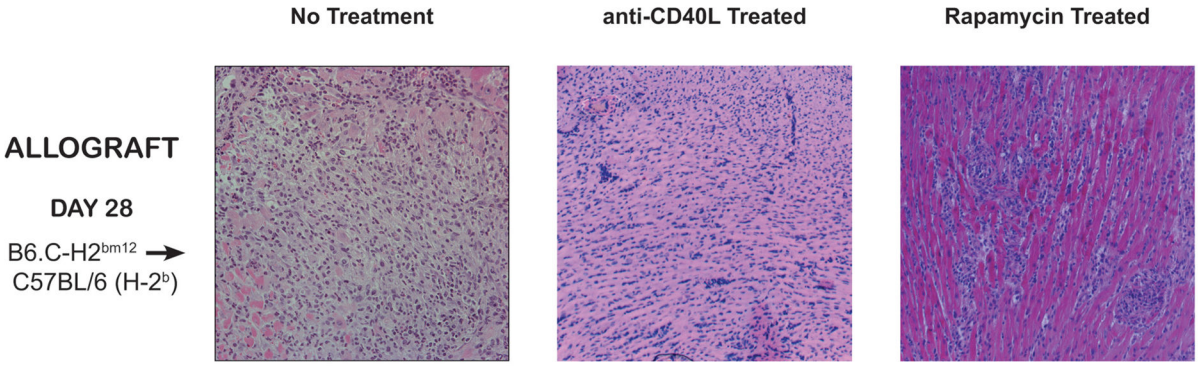

Figure 4.

Representative histology of transplanted hearts from allograft recipients on post-transplant day 28. The first panel shows diffuse leukocyte infiltration in an untreated animal (ISHLT Grade 3R), the second panel shows minimal leukocytic infiltrate in an animal treated with anti-CD40L (Grade 1R), and the third panel shows interstitial leukocytic infiltrate in an animal treated with low dose rapamycin (Grade 3R).

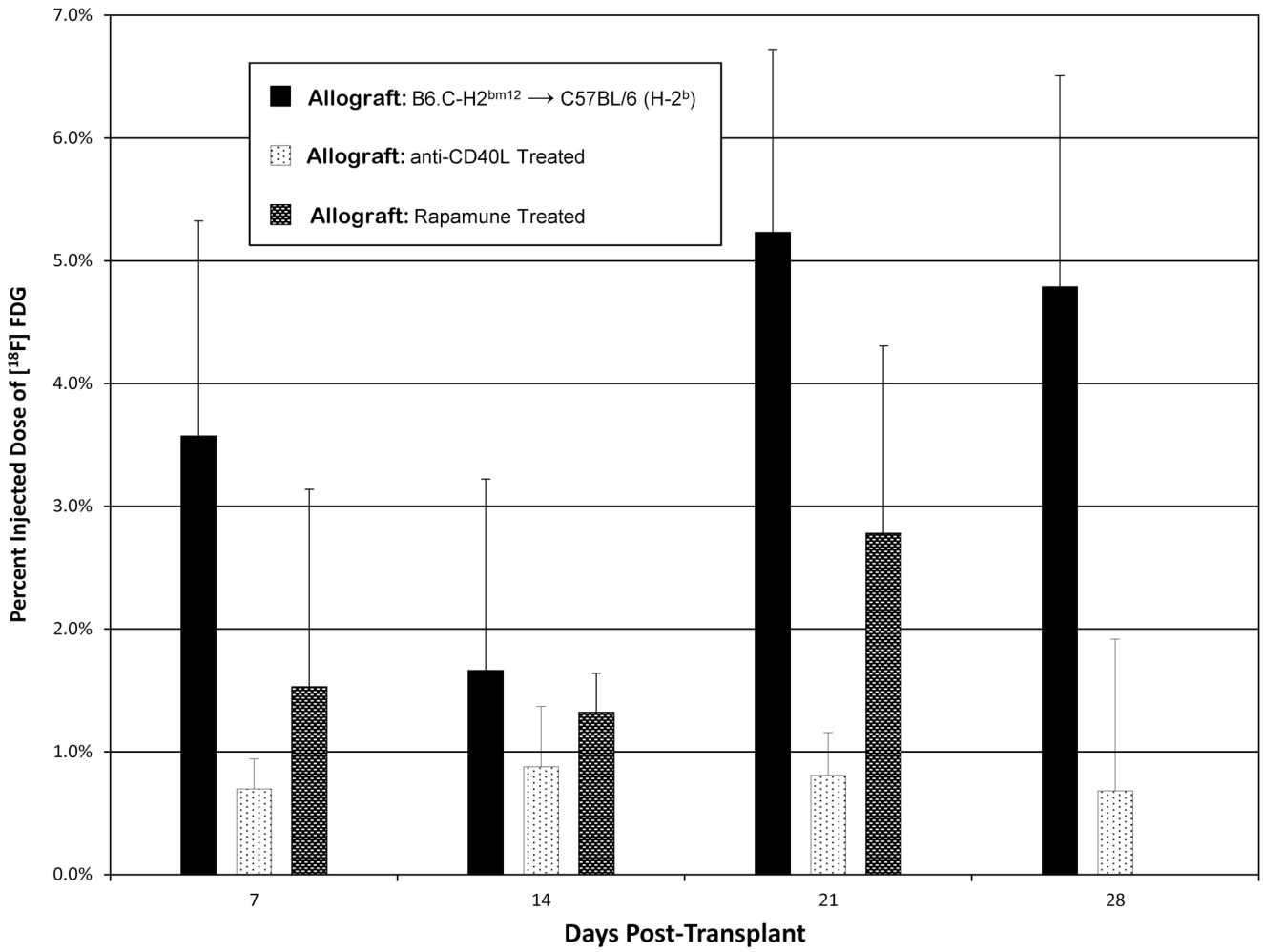

Figure 5.

The percent injected dose of [^{18}F]FDG within the transplanted allograft in untreated, anti-CD40L antibody treated, and rapamycin treated animals. Error bars represent the standard deviation of measurements within each group. [^{18}F]FDG uptake in allografts of anti-CD40L treated animals was significantly lower than untreated animals at each time point (P=0.006).